



Contents lists available at ScienceDirect

Bioorganic & Medicinal Chemistry Letters

journal homepage: www.elsevier.com/locate/bmcl

Design, synthesis, and biological evaluation of a scaffold for iGluR ligands based on the structure of (–)-kainocephalin

Rishi G. Vaswani^a, Agenor Limon^b, Jorge Mauricio Reyes-Ruiz^b, Ricardo Miledi^b, A. Richard Chamberlin^{a,c,*}

^a Department of Chemistry, University of California at Irvine, Irvine, CA 92697, USA

^b Department of Neurobiology and Behavior, University of California at Irvine, Irvine, CA 92697, USA

^c Department of Pharmaceutical Sciences, University of California at Irvine, Irvine, CA 92697, USA

ARTICLE INFO

Article history:

Received 1 September 2008

Revised 31 October 2008

Accepted 3 November 2008

Available online 6 November 2008

Keywords:

Kainocephalin

iGluR

Receptor antagonist

Excitatory amino acid receptor

AMPA receptor

KA receptor

Library scaffold

ABSTRACT

The design and synthesis of four pyrrolidine scaffolds that are structurally related to the known ionotropic glutamate receptor antagonist, (–)-kainocephalin, is described. Additionally, preliminary results of the biological evaluation of these compounds are disclosed.

© 2008 Elsevier Ltd. All rights reserved.

Small molecule libraries generated from scaffolds inspired by natural products have proven to be a rich source of new ligands for biological targets.¹ Our interest in natural product based libraries was motivated by our efforts to discover new ligands for the ionotropic glutamate receptors (iGluRs).² In addition to the central role iGluRs play in normal neuronal activation, their function is counterbalanced by a number of pathological processes.^{3–5} Excessive stimulation of the iGluRs by either L-glutamate (L-Glu) itself or by any of a large number of iGluR agonists can trigger a cascade of detrimental cellular events that ultimately lead to neuronal injury or death. This abnormal response to iGluR activation, known as excitotoxicity, is postulated to play a role in a variety of neurodegenerative disorders including epilepsy,^{4,5} Parkinson's disease,⁴ and Alzheimer's disease.⁴ It is therefore not surprising that there is a good deal of interest in discovering new small molecules that modulate iGluR function.

As one element of our search for iGluR antagonists, we envisioned the construction of a library based on a scaffold that emulates (–)-kainocephalin (**1**),⁶ one of the few natural iGluR ligands with antagonist activity. Stimulated by the current interest in using specific substructures found within natural products as library scaffolds, the C1–C7 segment of (–)-kainocephalin (**1**) was chosen as the template for library synthesis. Since appropriately

substituted aryl groups are commonly employed for introducing diversity elements in library synthesis, for example, via palladium-mediated cross-coupling reactions between aryl halides and boronates, we considered the 5-aryl pyrrolidine **2** as a possible scaffold (Fig. 1) for library synthesis.

This structure retains some of the glutamate-like structural elements known to be required for activity,⁷ while the phenyl ring would provide up to five positions for attaching the diversity elements when appropriately functionalized (halide, triflate, etc.) for aryl cross-coupling. The fairly substantial structural difference between **2** and **1** was, however, cause for some concern.

As a result, before proceeding we decided to study the unsubstituted core structure **2**, beginning with molecular modeling studies

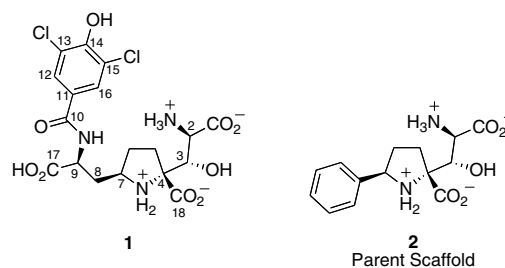


Figure 1. (–)-Kainocephalin (**1**) and targeted parent aryl-appended scaffold **2**.

* Corresponding author. Tel./fax: +1 949 824 6478.

E-mail address: archambe@uci.edu (A.R. Chamberlin).

to assess whether the proposed simplified scaffold might be a reasonable ligand for the iGluRs. Although one might argue that docking the natural product should come first, we chose to begin with the much simpler **2**, more or less as a model for **1**, which has many more degrees of rotational freedom and is a more difficult modeling problem. A further complication is that it is not at all obvious—in contrast to most glutamate-like iGluR ligands—how the highly functionalized kaitocephalin core might be oriented in the binding site. There clearly are two ‘embedded glutamates’ within this substructure that might control the ligand orientation, that is, one in which the C-2 nitrogen mimics the glutamate α -amino group, and a very different arrangement in which the pyrrolidine ring nitrogen does so (similar to kainate; see below). If that issue could be resolved, molecular modeling of **2** might provide information concerning which positions of the aryl ring might best tolerate the presence of substituents, which would in turn be instructive for our later library design. The parent scaffold **2** was therefore docked into the glutamate binding cleft of Gouaux’s X-ray structure of the iGluR2-kainate construct (Fig. 2)⁸ in these two starting orientations, and others. The resultant minimized structures indicated that the complex in which the scaffold pyrrolidine ring is oriented similarly to that of kainate produced the lowest energy structures. In these, the phenyl ring was readily accommodated in the binding site, with one of the *ortho*-positions directed towards the mouth of the binding cleft and therefore likely to be amenable to substitution (yellow arrow in Fig. 2). The other aryl positions appear to be either more sterically encumbered or buried.

The model shown in Figure 2 provided some reassurance that structures such as **2** might act as acceptable surrogates for (–)-kaitocephalin (**1**) and, with suitable aryl substituents, as library scaffolds; further, it also suggested that the *ortho*-position of the aryl ring would best tolerate substituents in such libraries. We should emphasize that although this is a simplistic analysis it does provide a testable hypothesis regarding where the diversity elements should eventually be attached to the phenyl ring, or more directly *not* be attached because of steric constraints; further modeling will be required to identify potentially favorable binding interactions between the substituents and residues in the binding site. As an initial experimental assessment of this model, particularly the steric tolerances at the different positions of the aryl ring, three additional steric probes were envisioned in addition to the parent scaffold (Fig. 3): the *ortho*-, *meta*-, and *para*-substituted tolyl derivatives **3**, **4**, and **5**, respectively, with the *ortho*-tolyl analog **3** predicted to be a better ligand than the *meta*- and *para*-counterparts, according to the model. To investigate these computational

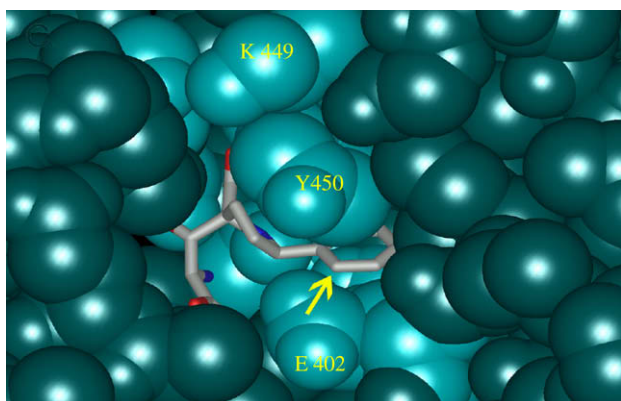


Figure 2. Docking of parent scaffold **2** into Gouaux’s iGluR2 construct. See text for details.

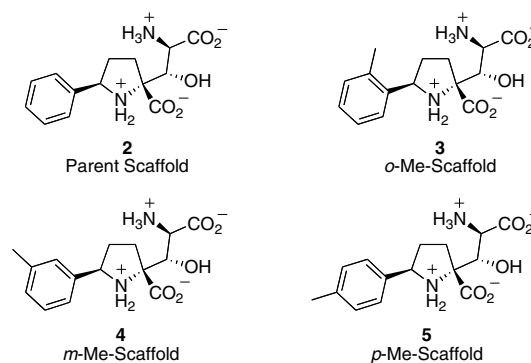


Figure 3. Targeted analogs based on modeling predictions.

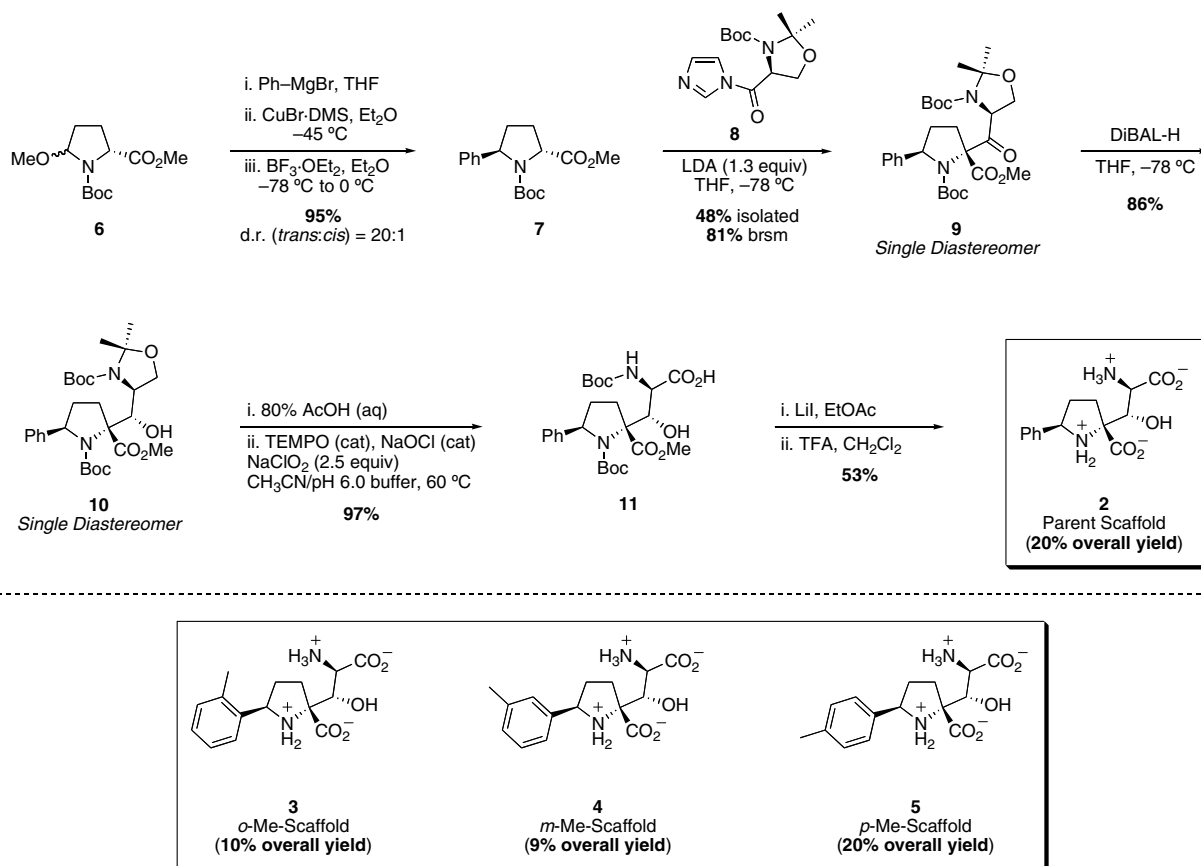
predictions, analogs **2**, **3**, **4**, and **5** were synthesized and submitted to biological evaluation.

The ultimate success of this library approach depends on the development of an expedient, efficient, and scalable synthetic strategy to access the various aryl substituted scaffolds. The specific route chosen for preparing the parent library scaffold **2** (Scheme 1) evolved from the principles established in our recent synthesis of (–)-kaitocephalin,⁹ in both cases utilizing primarily substrate-controlled manipulations for the iterative installation of the requisite stereocenters. We envisioned the construction of an enantiomerically pure 2,5-disubstituted pyrrolidine core to which the remaining carbon framework would be appended. A key element of the plan was to exploit the inherent functionality present in the synthetic intermediate to differentiate the multiple functional groups, thereby avoiding extensive protecting group manipulations.

To test the feasibility of this approach we constructed the parent scaffold **2** commencing with the formation of the requisite phenyl incorporated *trans*-2,5-disubstituted pyrrolidine ring. Of the various established methods for the construction of 2,5-disubstituted pyrrolidine rings,¹⁰ we chose the addition of organocopper reagents to the chiral *N*-acyliminium ion (derived from (*R*)-pyroglutamic acid). To implement this approach required the formation of amination **6**, which was chemically derived in three steps from (*R*)-pyroglutamic acid.⁹ Once amination **6** was in hand, transmetalation of phenyl Grignard with a suspension of CuBr·DMS in Et₂O, formed the desired organocopper species. Subsequent addition of BF₃·OEt₂ and the *N*-acyliminium precursor **6** produced **7** as a 20:1 mixture of diastereomers (*trans*:*cis*) in 95% yield.¹¹

Further functionalization to give the desired pyrrolidine substitution pattern next required the stereoselective introduction of the tetrasubstituted C4, followed by formation the C3 secondary alcohol. The formation of the tetrasubstituted center was established with excellent diastereoselectivity via a Claisen condensation of the lithium enolate derived from **7** and *N*-acylimidazole **8**,⁹ producing the β -keto ester **9** in 48% yield as a single detectable diastereomer. After an exhaustive investigation of reducing agents the diastereoselective reduction of the ketone **9** was achieved by employing DIBALH in THF to afford alcohol **10** as a single diastereomer in 86% yield, again with no evidence of the undesired diastereomer.

Hydrolysis of the *N,O*-acetonide was accomplished next with 80% aqueous AcOH and subsequent chemoselective TEMPO-catalyzed oxidation of the resultant primary alcohol furnished carboxylic acid **11** in 97% yield.¹² Deprotection of the methyl ester was effected with LiI¹³ in hot EtOAc and treatment with TFA in CH₂Cl₂ removed the Boc carbamates; reverse phase HPLC purification of the crude reaction mixture furnished **2** as the *bis*-trifluoroacetate ammonium salt in 53% yield.¹⁴ The *o*-tolyl, *m*-tolyl, and *p*-tolyl scaffolds, **3**,¹⁵ **4**,¹⁶ and **5**,¹⁷ respectively, were synthesized in an



Scheme 1. Synthesis of parent scaffold **2** and the *ortho*-, *meta*-, and *para*-tolyl analogs **3**, **4**, and **5**, respectively.

analogous sequence by substituting the appropriate tolyl-Grignard for the organocuprate reaction in the initial arylation of the *N*-acyliminium precursor **6**. This sequence should provide an expedient and efficient method for the eventual preparation of various substituted aryl scaffolds for library synthesis, and in the current application provided sufficient quantities of each of the four analogs for biological evaluation.

The activities of the parent compound **2** and its methyl analogs (**3**, **4**, and **5**) were screened in oocytes injected with mRNA from rat cerebral cortex.¹⁸ Potential AMPA/KA receptor antagonist activity was assayed based on the membrane current inhibition at a concentration of 100 μM for each analog against 100 μM of kainate as the control. Experiments were quite reproducible in multiple oocyte preparations ($N = 7$), generally with a standard error of a few percent.

In the antagonist activity assay (Fig. 4), the parent phenyl scaffold **2** proved to be a reasonably potent antagonist that reduces the kainate control current by approximately 28% (to 72% of control) at a concentration of 100 μM . The *ortho*-, *meta*-, and *para*-methyl substituted phenyl scaffolds, **3**, **4**, and **5**, respectively, also showed activity in antagonizing 100 μM kainate currents. Significantly, from the perspective of our binding model (Fig. 2), the *ortho*-methyl substituted phenyl scaffold **3** was more potent than either of the other methyl substituted analogs: the *meta*- and *para*-methyl substituted phenyl scaffolds, **4** and **5** reduced kainate control current by approximately 25% ($75 \pm 5\%$ of control) and 17% ($83 \pm 6\%$ of control), respectively, while the *ortho*-methyl substituted phenyl scaffold **3** reduced kainate current by half ($49 \pm 6\%$ of control). None of the analogs showed agonist activity on AMPA/KA receptors when tested alone at concentrations of 100 μM ($N = 5$).

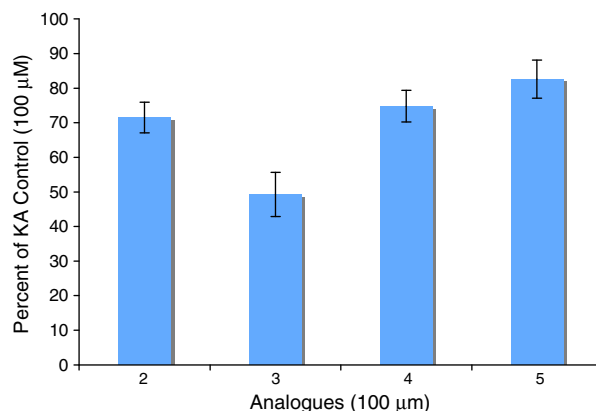


Figure 4. Antagonist activity assay of compounds **2**, **3**, **4**, and **5**, respectively. See text for conditions.

It was gratifying that initial screening of the analogs **2**, **3**, **4**, and **5** revealed a reasonable level of antagonist activity (Fig. 4) for each, with the most active of the group, **3**, exhibiting a potency comparable to kainate itself (albeit as an antagonist, in contrast to the agonist activity of kainate). In addition, the relative potencies of the four compounds are consistent with the modeling predictions suggesting that the *ortho*-position of the aryl ring should tolerate additional steric bulk well and thus may be the preferred point of attachment of diversity elements in future libraries, while analogs with substituents in the *meta*- and the *para*-positions may be less potent because of greater respective steric constraints in the binding site. Although the results obtained from the initial

screen are far from comprehensive, they provide considerable additional motivation for the development of these kaitocephalin-inspired scaffolds as novel iGluR antagonists.

Acknowledgments

We are grateful for support from the National Institute of Neurological Disorders and Stroke (NS-27600 to A.R.C.) and from the American Health Assistance Foundation (A2006-054 to R.M.).

References and notes

- (a) Messer, R.; Fuhrer, C.; Haner, R. *Curr. Opin. Chem. Biol.* **2005**, *9*, 259; (b) Shang, S.; Tan, D. *Curr. Opin. Chem. Biol.* **2005**, *9*, 248; (c) Lee, M.-L.; Schneider, G. L. *J. Comb. Chem.* **2001**, *10*, 284; (d) Nicolaou, K. C.; Pfefferkorn, J. A.; Cao, G. Q.; Barluenga, S.; Mitchell, H. J. *J. Am. Chem. Soc.* **2000**, *122*, 9939.
- (a) Cohen, J. L.; Limon, A.; Miledi, R.; Chamberlin, A. R. *Bioorg. Med. Chem. Lett.* **2006**, *16*, 2189; (b) Shou, X.; Miledi, R.; Chamberlin, A. R. *Bioorg. Med. Chem. Lett.* **2005**, *15*, 3942.
- (a) Gill, A.; Madden, D. R.; Royal Chemical Society: Cambridge, UK, 2006.; (b) Trist, D. G. *Pharm. Acta Helv.* **2000**, *74*, 221; (c) Bleakman, D.; Logdge, D. *Neuropharmacology* **1998**, *37*, 1187.
- (a) Doble, A. *Pharmacol. Ther.* **1999**, *81*, 163; (b) Löscher, W. *Prog. Neurobiol.* **1998**, *54*, 721.
- Brauner-Osborne, H.; Egebjerg, J.; Nielsen, E. O.; Madsen, U.; Krosggaard-Larsen, P. *J. Med. Chem.* **2000**, *43*, 2609.
- (a) Shin-ya, K.; Kim, J.-S.; Furihata, K.; Hayakawa, Y.; Seto, H. *Tetrahedron Lett.* **1997**, *38*, 7079; (b) Kobayashi, H.; Shin-ya, K.; Furihata, K.; Hayakawa, Y.; Seto, H. *Tetrahedron Lett.* **2001**, *42*, 4021; (c) Kobayashi, H.; Shin-ya, K.; Furihata, K.; Hayakawa, Y.; Seto, H.; Watanabe, H.; Kitahara, T. *Tetrahedron Lett.* **2002**, *43*, 853.
- Watkins, J. C.; Krosggaard-Larsen, P.; Honoré, T. *Trends Pharmacol. Sci.* **1990**, *11*, 25.
- Molecular modeling was performed in collaboration with Dr. Xiaohong Shou. Molecular dynamics and minimizations of the ligand/iGluR2S1S2 construct complex were carried out on a Silicon Graphics Octane 2 computer using the Discover _3 module on Insight II version 2002. Dynamics were carried out at 300 K. Only the residues of the S1S2 construct within 7.0 Å of the docked ligand were allowed to relax during the minimization and dynamics simulation.
- Vaswani, R. G.; Chamberlin, A. R. *J. Org. Chem.* **2008**, *73*, 1661.
- Pichon, M.; Figadere, B. *Tetrahedron: Asymmetry* **1996**, *7*, 927.
- (a) Wistrand, L. G.; Skrinjar, M. *Tetrahedron* **1991**, *47*, 573; (b) Collado, I.; Ezquerra, J.; Pedregal, C. *J. Org. Chem.* **1995**, *60*, 5011; (c) Thaning, M.; Wistrand, L. G. *Acta Chem. Scand.* **1992**, *46*, 194; (d) Ludwig, C.; Wistrand, L. G. *Acta Chem. Scand.* **1994**, *48*, 367; (e) Ludwig, C.; Wistrand, L. G. *Acta Chem. Scand.* **1990**, *44*, 707; (f) Skrinjar, M.; Wistrand, L. G. *Tetrahedron Lett.* **1990**, *31*, 1775.
- Zhao, M.; Li, J.; Mano, E.; Song, Z.; Tschäen, D. M.; Grabowski, E. J. J.; Reider, P. J. *J. Org. Chem.* **1999**, *64*, 2564.
- Fisher, J. W.; Trinkle, K. L. *Tetrahedron Lett.* **1994**, *35*, 2505.
- Characterization for **2**: ¹H NMR (500 MHz, D₂O/CH₃CN (10:1), 315 K) δ 7.79–7.72 (m, 5H), 5.01 (dd, *J* = 12.1, 5.6, 1H), 4.85 (br s, 1H), 4.68 (br s, 1H), 2.85 (dd, *J* = 12.1, 5.7, 1H), 2.69–2.54 (m, 1H and dd, *J* = 13.2, 5.9), 2.45 (qd, *J* = 12.2, 6.2); ¹³C NMR (100 MHz, D₂O, uncalibrated) δ 173.7, 170.6, 134.4, 130.0, 129.6, 128.0, 76.7, 70.5, 64.5, 55.7, 33.0, 30.3; HRMS (ESI/methanol) *m/z* Calcd for C₁₄H₁₈N₂O₅ (M+Na)⁺ 317.1113. Found 317.1104; [α]_D²⁵ –18.5° (c 0.11, H₂O).
- Characterization for **3**: ¹H NMR (500 MHz, D₂O) δ 7.58–7.54 (m, 1H), 7.37–7.31 (m, 3H), 5.03 (dd, *J* = 12.2, 5.5, 1H), 4.62 (s, 1H), 4.48 (s, 1H), 2.60 (dd, *J* = 12.4, 5.9, 1H), 2.42 (s, 3H), 2.38–2.31 (m, 2H), 2.28–2.19 (m, 1H); ¹³C NMR (125 MHz, D₂O, uncalibrated) δ 173.8, 170.6, 137.8, 132.4, 131.0, 129.6, 127.0, 126.3, 76.7, 70.4, 59.9, 55.5, 32.8, 29.4, 18.6; HRMS (ESI/methanol) *m/z* Calcd for C₁₅H₂₀N₂O₅ (M+Na)⁺ 331.1270. Found 331.1265; [α]_D²⁵ –42.3° (c 0.11, H₂O).
- Characterization for **4**: ¹H NMR (500 MHz, D₂O) δ 7.39–7.35 (m, 2H), 7.31–7.29 (m, 2H), 4.71 (dd, *J* = 12.5, 5.3, 1H), 4.64 (s, 1H), 4.47 (s, 1H), 2.62–2.58 (m, 1H), 2.40–2.32 (m, 2H and s, 3H), 2.21–2.14 (m, 1H); ¹³C NMR (125 MHz, D₂O, uncalibrated) δ 173.4, 170.3, 139.7, 134.1, 130.5, 129.33, 128.3, 124.7, 76.3, 70.2, 64.3, 55.4, 32.8, 30.1, 20.4; HRMS (ESI/methanol) *m/z* Calcd for C₁₅H₂₀N₂O₅ (M+H)⁺ 309.1451. Found 309.1450; [α]_D²⁵ –24.2° (c 0.10, H₂O).
- Characterization for **5**: ¹H NMR (500 MHz, D₂O) δ 7.42 (app d, *J* = 8.2, 2H), 7.32 (app d, *J* = 7.9, 2H), 4.73 (dd, *J* = 12.1, 5.4, 1H), 4.60 (d, *J* = 0.85, 1H), 4.51 (s, 1H), 2.60–2.56 (m, 1H), 2.40–2.30 (m, 2H and s, 3H), 2.21–2.13 (m, 1H); ¹³C NMR (125 MHz, D₂O, uncalibrated) δ 173.7, 170.5, 140.3, 131.2, 129.9, 127.7, 76.4, 70.4, 64.1, 55.5, 32.8, 30.1, 20.3; HRMS (ESI/methanol) *m/z* calcd for C₁₅H₂₀N₂O₅ (M+H)⁺ 309.1451. Found 309.1445; [α]_D²⁵ –23.8° (c 0.12, H₂O).
- Gundersen, C. B.; Miledi, R.; Parker, I. *Proc. R. Soc. B., Biol. Sci.* **1984**, *221*, 127.